Structure 14, 1723–1727, November 2006 ©2006 Elsevier Ltd All rights reserved DOI 10.1016/j.str.2006.09.007

Determinants of Bacteriophage ϕ29 Head Morphology

Kyung H. Choi,[1] Marc C. Morais,[1] Dwight L. Anderson,[2] and Michael G. Rossmann[1,*]
[1] Department of Biological Sciences
Purdue University
915 West State Street
West Lafayette, Indiana 47907
[2] Departments of Microbiology and Diagnostic and Biological Science
University of Minnesota
18-242 Moos Tower
Minneapolis, Minnesota 55455

Summary

Bacteriophage ϕ29 requires scaffolding protein to assemble the 450 × 540 Å prolate prohead with $T = 3$ symmetry end caps. In infections with a temperature-sensitive mutant scaffolding protein, capsids assemble predominantly into 370 Å diameter isometric particles with $T = 3$ symmetry that lack a head-tail connector. However, a few larger, 430 Å diameter, particles are also assembled. Cryo-electron microscopy shows that these larger particles are icosahedral with $T = 4$ symmetry. The prolate prohead, as well as the two isometric capsids with $T = 3$ and $T = 4$ symmetry, are composed of similar pentamers and differently skewed hexamers. The skewing of the hexamers in the equatorial region of proheads and in the $T = 4$ isometric particles reflects their different environments. One of the functions of the scaffolding protein, present in the prohead, may be to stabilize skewed hexamers during assembly.

Introduction

Double-stranded DNA (dsDNA) bacteriophages utilize scaffolding proteins to ensure proper sequential conformational changes of subunits during capsid assembly (Dokland, 1999; Fane and Prevelige, 2003). Assembly in the presence of defective scaffolding proteins results in particles that are aberrant in shape and size. For instance, bacteriophages P22, P2, and lambda form icosahedral $T = 7$ capsid structures in the presence of scaffolding protein (Dokland et al., 1992; Dokland and Murialdo, 1993; Thuman-Commike et al., 1996). In the absence of its scaffolding proteins, P22 forms smaller, $T = 4$, particles (Thuman-Commike et al., 1999). In the P2-P4 bacteriophage system, the presence of the P4 protein gpSid causes the P2 capsid protein to assemble into smaller, $T = 4$, capsids instead of $T = 7$ capsids (Dokland et al., 1992; Shore et al., 1978). In the *Bacillus subtilis* bacteriophage ϕ29, scaffolding protein is necessary for elongation of the prolate head (Anderson and Reilly, 1993; Hagen and Anderson, 1975).

The first particles assembled during ϕ29 morphogenesis are proheads, which are composed of the scaffolding protein gp7, the capsid protein gp8, the head fiber protein gp8.5, the connector protein gp10, and a phage-encoded, 174 base RNA (pRNA) (Anderson and Reilly, 1993). The viral genome is then packaged into the prohead with the aid of a ϕ29-encoded ATPase, gp16, and the scaffolding protein exits. Upon completion of DNA packaging, ATPase and pRNA are released, and the lower collar, appendages, tail axis, and tail knob are attached to form the mature virion. The phage head is elongated along a 5-fold symmetry axis, and the arrangement of subunits on the surface of the phage can be described by the triangulation numbers of $T = 3$, $Q = 5$ (Tao et al., 1998).

Restrictive infection with suppressor-sensitive (*sus*) or temperature-sensitive (*ts*) ϕ29 mutants in either the scaffolding protein or the head-tail connector results in aberrant particles and spherical isometric particles, respectively (Hagen et al., 1976; Morais et al., 2005; Tao et al., 1998). Although the majority of the particles assembled in the presence of mutant scaffolding protein have $T = 3$ symmetry, a small portion of particles assemble into larger spherical capsids. We report here the structure of the larger isometric capsids determined by cryo-electron microscopy (cryo-EM). A three-dimensional reconstruction shows a $T = 4$ arrangement of the capsid subunits, but with only one trimeric fiber within each icosahedral asymmetric unit. Comparison of the capsomers in the prohead, $T = 3$, and the $T = 4$ particles suggests that the role of scaffolding protein could be to stabilize the skewed hexameric capsomers.

Results

Fibered isometric ϕ29 particles were produced in restrictive infections of *Bacillus subtilis* with the *ts* gp7 (224) mutant (here, 224 identifies the specific mutant). The majority of particles were $T = 3$ isometric icosahedra with a diameter of ~370 Å (Morais et al., 2005; Tao et al., 1998). However, ~10% of the particles had a larger diameter of ~430 Å (Figure 1), and a few particles were even larger. Based on the ratio of the surface areas to the number of subunits per particle and the fact that the smaller $T = 3$ particles contain 180 subunits (Tao et al., 1998), the larger isometric particles were predicted to have a $T = 4$ arrangement requiring 240 subunits. Specifically, the ratio of the square of their radii is 1.35, and the ratio of their T numbers is 1.33. Most of the particles did not contain DNA.

The larger particles were selected by eye. A three-dimensional reconstruction was calculated from 785 particles. The resolution of the resulting reconstruction extended to 20 Å, as determined by the difference Fourier shell correlation method. The moderately large number of particles used in the reconstruction that attained only 20 Å resolution suggests that there was some heterogeneity in the samples, as is seen in one of the indicated particles in Figure 1. The reconstructed particle has a diameter of 464 Å along the 3-fold axes and 430 Å along the 5-fold axes (Figure 2A). A projection of particle density corresponding to a 223 Å radius, along

*Correspondence: mr@purdue.edu

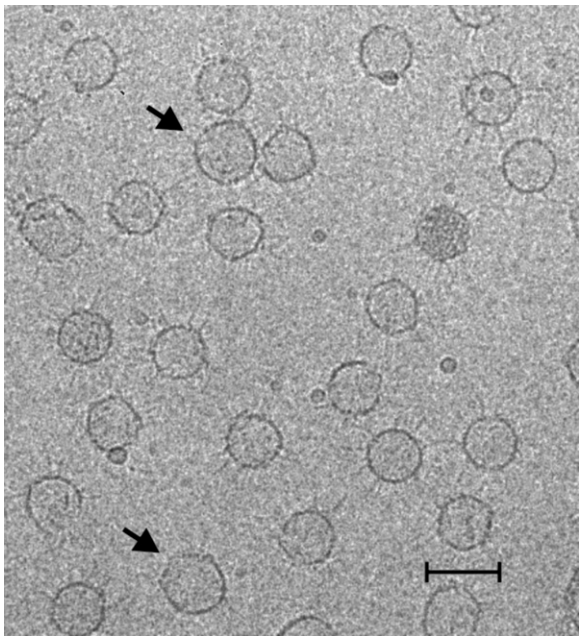

Figure 1. Cryo-EM Micrograph Showing ϕ29 Isometric Particles

The image is taken on an FEI CM200 microscope at a magnification of 39,500. *T* = 4 isometric particles are indicated with arrows to differentiate them from *T* = 3 particles. The scale bar corresponds to 500 Å.

an icosahedral 2-fold axis, shows a *T* = 4 subunit arrangement of pentamers and hexamers (Figure 2B).

The trimeric fibers are attached at quasi-3-fold axes, between two hexamers and one pentamer. Thus, the fibers are arranged with one trimeric fiber situated at each of the quasi-3-fold axes at the pentameric corners (Figure 3A), as is also the case in the *T* = 3 particles (Morais et al., 2005; Tao et al., 1998). Hence, regardless of the *T* number, the number of fibers will always be the same in isometric particles. Consistent with this result, fibers do not bind to the equatorial region of the prolate prohead where local 3-fold vertices are composed of three hexamers (Tao et al., 1998). The fiber protein consists of two domains, one forming the base and the other forming the fiber, which extends approximately radially (Morais et al., 2005; Tao et al., 1998). In contrast to the *T* = 3 particles, the density for the fibers in the *T* = 4 particles is weak, and even when contoured at 0.5σ, only the base of the fiber protein is visible. Since the pentamers protrude from the surface of the particle, the fiber directions are not completely radial.

Discussion

Comparison with *T* = 3 Particles

The structure of fibered, *T* = 3 isometric ϕ29 capsids had been determined by cryo-EM to 8.7 Å resolution (Figure 3B) (Morais et al., 2005). In the *T* = 3 icosahedral capsids, the quasi-6-fold axes of the hexamers coincide with the icosahedral 3-fold axes, and each hexamer is surrounded by three pentamers and three hexamers (Figure 4). Thus, there is only one type of quasi-3-fold axis relating two hexamers and one pentamer. In contrast, in *T* = 4 capsids, hexamers are located on the icosahedral 2-fold axes, and each hexamer is surrounded by two pentamers and four hexamers (Figure 4). As a consequence, there are two types of 3-fold axes relating capsomers. One type coincides with the icosahedral 3-fold axes and relates three hexamers, whereas the other type is a quasi-3-fold axis that relates two hexamers and a pentamer. Pentamers in the *T* = 3 and *T* = 4 capsids have almost identical dimensions, whereas hexamers in the *T* = 4 capsids are slightly skewed when compared to those in the *T* = 3 capsids (Figures 3A–3D); this skewing is similar to the conformational changes that occur in HK97 (Conway et al., 2001).

Comparison with the Structure of the Prolate Prohead

The arrangement of subunits in the ϕ29 prolate prohead can be described in terms of the *T* = 3 and *Q* = 5 triangulation numbers, where 30(*T* + *Q*) equals the number of monomers. The 52 symmetry breaks down at one end of the particle, where one pentamer is replaced by the head-tail connector. Thus, proheads contain 11 pentamers and 30 hexamers. In prolate proheads, as well as *T* = 3 or *T* = 4 isometric particles, pentamers are surrounded by a ring of five hexamers. Thus, the structures of pentamers in all of these particles are very similar.

Four different types of hexamers are observed in the prolate prohead, based on the environment of each hexamer (Morais et al., 2005). Hexamers in the icosahedral end cap interact with three pentamers and three hexamers (Type I, Figure 4). Hexamers in the equatorial region either interact with two pentamers and four hexamers

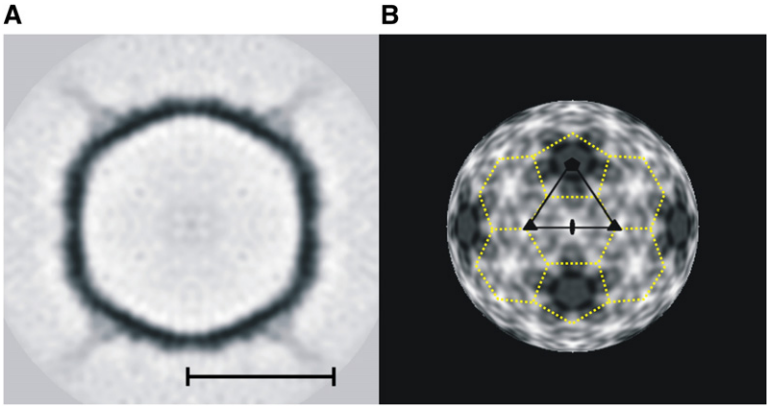

Figure 2. Cryo-EM Three-Dimensional Reconstruction of Fibered Isometric ϕ29 Particles

(A and B) (A) Central cross-section and (B) projection of the cryo-EM density at a radius of 223 Å viewed down an icosahedral 2-fold axis for the *T* = 4 particle. High-density features are dark, and low-density features have a lighter shade. The scale bar corresponds to 250 Å. The icosahedral asymmetric unit is shown as a black triangle, and 5-, 3-, and 2-fold axes are shown as a pentagon, triangles, and an oval, respectively. Some pentamers and hexamers are outlined in yellow in (B).

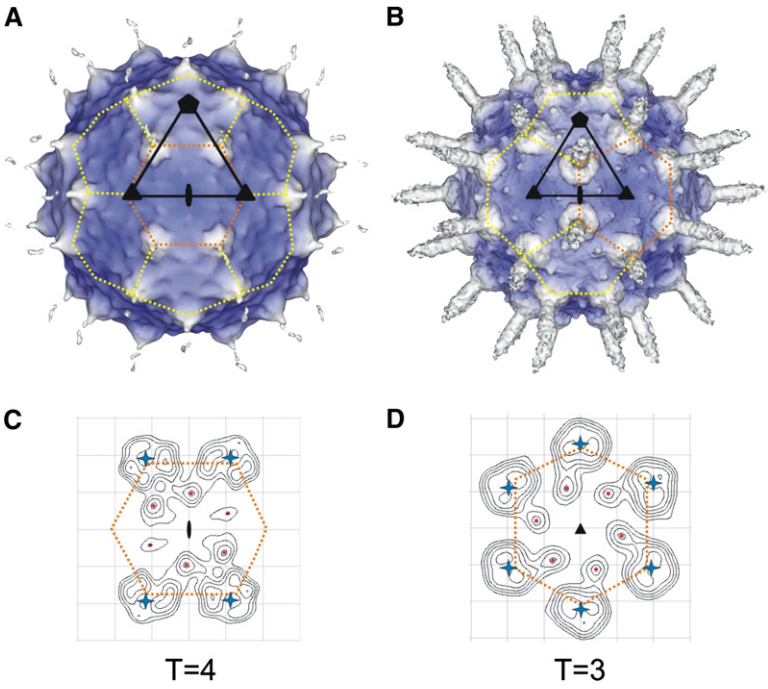

Figure 3. Comparison of the T = 4 and T = 3 Isometric Particles

(A) Surface-shaded representation of the T = 4 isometric particle viewed down an icosahedral 2-fold axis, contoured at 0.5σ to show the fibers. The surface is colored from blue to white with increasing radius. One hexamer is outlined in orange, and the other hexamers and pentamers are outlined in yellow.

(B) Surface-shaded reconstruction of the fibered T = 3 isometric particle shown for comparison with the T = 4 particle, also viewed down an icosahedral 2-fold axis contoured at 1σ.

(C) Contoured cross-section of a hexamer in the T = 4 isometric particle. The center of high-density features in the hexamer is indicated by a red dot. Contour lines are drawn starting at 0.5σ with a 0.4σ step size. Note that the distance across the hexamer is less for vertical separation than the other distances. The centers of the fibers are indicated with blue stars.

(D) Contoured cross-section of a hexamer in the T = 3 isometric particles. The contour lines are drawn from 1σ with a 0.5σ step size. Comparing hexamers in (C) and (D), it is apparent that the quasi-6-fold symmetry seen in (D) is reduced only to 2-fold symmetry in (C).

(Type II) or with one pentamer and five hexamers (Type III). Hexamers near the special vertex interact with three hexamers, two pentamers, and one connector (Type IV). In contrast, isometric particles display only one type of hexamer. Hexamers in T = 3 isometric particles reside at 3-fold symmetry axes and display quasi-6-fold symmetry. They have an environment similar to Type I hexamers in the prohead. Hexamers in T = 4 isometric particles are similar to Type II prohead hexamers in that they are surrounded by two pentamers and four hexamers. However, pentamers reside at *meta* positions for the Type II hexamers in the prohead (i.e., they are 120° apart), but they are in *para* positions in the T = 4 isometric particles (i.e., they are 180° apart). The hexamers in T = 4 isometric particles are slightly skewed, resulting in 2-fold symmetry instead of quasi-6-fold symmetry. Such a skewing is not possible in T = 3 particles, where hexamers sit on icosahedral 3-fold axes (Morais et al., 2005). Skewing of hexamers is also observed in Types II and III prohead hexamers. Type III hexamers of proheads are surrounded by one pentamer and five hexamers. Such an arrangement would occur in T = 7 particles, as, for instance, HK97 and P22. Isometric particles larger than T = 4 isometric heads were observed along with the T = 3 and T = 4 particles. Based on their radii, they are predicted to have T = 7 symmetry.

In summary, T = 3, T = 4, and T = 7 particles are assembled with 20, 30, and 60 hexamers of Types I, II, and III, respectively, together with 12 pentamers in each case. In contrast, the number of hexamers of Types I, II, III, and IV in ϕ29 proheads is 5, 10, 10, and 5, respectively. Ignoring the presence of the connector, Type IV hexamers have essentially the same environment as Type I hexamers; thus, there are only three types of hexameric environments.

Role of the Scaffolding Protein in ϕ29 Assembly

In the presence of mutant scaffolding protein, most of the assembled particles have T = 3 symmetry utilizing Type I hexamers, indicating that T = 3 assembly is either the most stable or the most accessible arrangement of subunits. There is a smaller number of Type II-like hexamers that assemble into T = 4 icosahedral particles. Thus, the scaffolding protein must provide the means for producing the most skewed Type III hexamers, which are observed only in the prolate capsids assembled in the presence of wild-type scaffolding protein. Hence, a plausable hypothesis is that assembled hexamers have an innate ability to skew (as seen in the slightly skewed Type II hexamers) and that the function of the wild-type scaffolding protein (or the mutant scaffolding protein at permissive temperatures) is to facilitate and

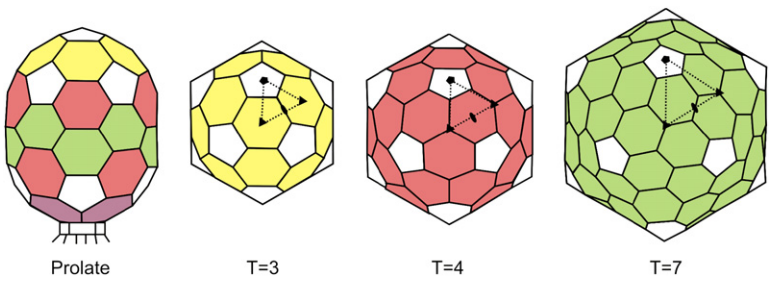

Figure 4. Triangulation Net of the Prolate ϕ29 Head and the T = 3 Isometric, T = 4 Isometric, and Hypothetical T = 7 Isometric Particles

Type I, II, III, and IV hexamers are shown in yellow, red, green, and purple, respectively.

enhance the ability to skew. The various types of quasi-symmetrical properties of the nonskewed (Type I), mildly skewed (Type II), and highly skewed (Type III) hexamers may help direct the self-assembly of the various observed particles (Figure 4).

The mutant virus used here was found to have a defect in the scaffolding protein, where Ser65 was mutated to Asn (D.L.A., unpublished data). The crystal structure of the ϕ29 scaffolding protein shows that this site is at the interface between two dimers, thus inhibiting the formation of the normal scaffolding protein lattice during assembly of the prohead (Morais et al., 2003). Apparently, this lattice is critical for the formation of skewed hexamers in the assembly process.

The three-dimensional cryo-EM reconstruction reported by Morais et al. (2003) is consistent with this hypothesis. It showed that the scaffolding protein is located primarily in the equatorial section of the prohead and coincides most strongly with Type III hexamers (Morais et al., 2005), indicating specific interactions between scaffolding proteins and Type III hexamers and, to a lesser extent, with Type II hexamers.

It would seem reasonable to assume that the greater the skewing, the greater the need for scaffolding protein. Hence, in the presence of mutant scaffolding protein at nonpermissive temperatures, Type I hexamers (no skewing) would be the most abundant, and Type III hexamers would be the least frequent. This would account for T = 3 particles (with Type I hexamers) being the most frequent, T = 4 particles (with Type II-like hexamers) being more rare, and T = 7 particles (suspected of having Type III hexamers) being the rarest in assembly in the absence of wild-type scaffolding protein. Similarly, bacteriophage P22 assembles into T = 7 particles in the presence of scaffolding protein, whereas the absence of scaffolding protein results in predominantly T = 4 particles (Earnshaw and King, 1978; Thuman-Commike et al., 1999). Furthermore, when bacteriophages HK97 and P22 mature into infectious particles and lose their scaffolding protein, their skewed hexameric capsomers gain good 6-fold symmetry. However, the degree of skewedness is the same for the P22 hexamers in the T = 4 and T = 7 particles, demonstrating that the hexamers, even without scaffolding protein, have a tendency to skew.

Thus, the hexamers in bacteriophage ϕ29 are likely to exist as an equilibrium between different states of skewedness. In the presence of mutant protein at nonpermissive temperatures, this equilibrium favors the nonskewed hexamers with a minority of Type II and an even smaller amount of Type III hexamers. The relative number of these types of hexamers may partially account for the number of isometric particles assuming T = 3, T = 4, and predicted T = 7 geometry. The role of the scaffolding protein may be to shift the equilibrium toward the skewed hexamers necessary for the assembly of the prolate T = 3, Q = 5 head.

Experimental Procedures

Particle Preparation and Cryo-EM Reconstruction

Sample preparation and electron microscopy of the fibered isometric ϕ29 particles have been described previously (Wichitwechkarn et al., 1989). Briefly, *B. subtilis* RD2 (*sup*$^-$) was infected with the mutant *ts* 7 (224)-*sus* 16 (300)-*sus* 14 (1241) at 45°C. This mutant has Asn in place of Ser at position 65 in its scaffolding protein (D.L.A., unpublished data).

T = 4 particles from micrographs were selected by eye based on their larger apparent diameters. The initial reconstruction of the T = 4 isometric particles was generated by EMAN (Ludtke et al., 1999), assuming only icosahedral symmetry, but with no assumptions regarding T numbers. About 10% of the boxed particles were selected for the best 5-fold, 3-fold, and 2-fold views, and a three-dimensional image was reconstructed from class averages for each of these three views. After refinement with the program EMAN, an improved reconstruction was then used for polar Fourier transform orientation searches and subsequent reconstruction with the P3DR program (Baker and Cheng, 1996). Orientations were further refined by using the POR program (Ji et al., 2003). Contrast transfer function parameters were determined by using the program RobEM (http://cryoem.ucsd.edu/programs.shtm), and phases and amplitudes were corrected during the reconstruction process.

The number of particles used in the final reconstruction was 785 of a total of 1609 boxed particles. The resolution of the final map was estimated to be 20 Å by the Fourier shell correlation coefficient method with 0.5 as the cutoff criterion.

Acknowledgments

We thank Cheryl Towell and Sharon Wilder for help in the preparation of this manuscript and Norm Olson for taking the original micrographs of the isometric particles. We thank Jaya S. Koti for helpful discussions. This research was supported by National Science Foundation grant MCB0443899 to M.G.R. and a National Institutes of Health grant DE003606 to D.L.A.

Received: April 25, 2006
Revised: September 12, 2006
Accepted: September 19, 2006
Published: November 14, 2006

References

Anderson, D., and Reilly, B. (1993). Morphogenesis of bacteriophage ϕ29. In *Bacillus subtilis* and Other Gram-Positive Bacteria: Biochemistry, Physiology, and Molecular Genetics, A.L. Sonenshein, J.A. Hoch, and R. Losick, eds. (Washington, D.C.: American Society for Microbiology), pp. 859–867.

Baker, T.S., and Cheng, R.H. (1996). A model-based approach for determining orientations of biological macromolecules imaged by cryoelectron microscopy. J. Struct. Biol. *116*, 120–130.

Conway, J.F., Wikoff, W.R., Cheng, N., Duda, R.L., Hendrix, R.W., Johnson, J.E., and Steven, A.C. (2001). Virus maturation involving large subunit rotations and local refolding. Science *292*, 744–748.

Dokland, T. (1999). Scaffolding proteins and their role in viral assembly. Cell. Mol. Life Sci. *56*, 580–603.

Dokland, T., and Murialdo, H. (1993). Structural transitions during maturation of bacteriophage lambda capsids. J. Mol. Biol. *233*, 682–694.

Dokland, T., Lindqvist, B.H., and Fuller, S.D. (1992). Image reconstruction from cryo-electron micrographs reveals the morphopoietic mechanism in the P2–P4 bacteriophage system. EMBO J. *11*, 839–846.

Earnshaw, W., and King, J. (1978). Structure of phage P22 coat protein aggregates formed in the absence of the scaffolding protein. J. Mol. Biol. *126*, 721–747.

Fane, B.A., and Prevelige, P.E., Jr. (2003). Mechanism of scaffolding-assisted viral assembly. Adv. Protein Chem. *64*, 259–299.

Hagen, E.W., and Anderson, D.L. (1975). *In situ* lysis of ϕ29- and SPOI-infected *Bacillus subtilis*. J. Virol. *15*, 217–220.

Hagen, E.W., Reilly, B.E., Tosi, M.E., and Anderson, D.L. (1976). Analysis of gene function of bacteriophage ϕ29 of *Bacillus subtilis*: identification of cistrons essential for viral assembly. J. Virol. *19*, 501–517.

Ji, Y., Marinescu, D.C., Zhang, W., and Baker, T.S. (2003). Orientation refinement of virus structures with unknown symmetry. Paper

presented at: Proceedings of the 17th International Parallel and Distributed Processing Symposium (IEEE Computer Society).

Ludtke, S.J., Baldwin, P.R., and Chiu, W. (1999). EMAN: semiautomated software for high-resolution single-particle reconstructions. J. Struct. Biol. *128*, 82–97.

Morais, M.C., Kanamaru, S., Badasso, M.O., Koti, J.S., Owen, B.A., McMurray, C.T., Anderson, D.L., and Rossman, M.G. (2003). Bacteriophage ϕ29 scaffolding protein gp7 before and after prohead assembly. Nat. Struct. Biol. *10*, 572–576.

Morais, M.C., Choi, K.H., Koti, J.S., Chipman, P.R., Anderson, D.L., and Rossmann, M.G. (2005). Conservation of the capsid structure in tailed dsDNA bacteriophages: the pseudoatomic structure of ϕ29. Mol. Cell *18*, 149–159.

Shore, D., Deho, G., Tsipis, J., and Goldstein, R. (1978). Determination of capsid size by satellite bacteriophage P4. Proc. Natl. Acad. Sci. USA *75*, 400–404.

Tao, Y., Olson, N.H., Xu, W., Anderson, D.L., Rossmann, M.G., and Baker, T.S. (1998). Assembly of a tailed bacterial virus and its genome release studied in three dimensions. Cell *95*, 431–437.

Thuman-Commike, P.A., Greene, B., Jakana, J., Prasad, B.V.V., King, J., Prevelige, P.E., Jr., and Chiu, W. (1996). Three-dimensional structure of scaffolding-containing phage P22 procapsids by electron cryo-microscopy. J. Mol. Biol. *260*, 85–98.

Thuman-Commike, P.A., Greene, B., Malinski, J.A., Burbea, M., McGough, A., Chiu, W., and Prevelige, P.E., Jr. (1999). Mechanism of scaffolding-directed virus assembly suggested by comparison of scaffolding-containing and scaffolding-lacking P22 procapsids. Biophys. J. *76*, 3267–3277.

Wichitwechkarn, J., Bailey, S., Bodley, J.W., and Anderson, D. (1989). Prohead RNA of bacteriophage ϕ29: size, stoichiometry and biological activity. Nucleic Acids Res. *17*, 3459–3468.

Accession Numbers

A three-dimensional cryo-EM map has been deposited in the European Bioinformatics Institute with accession code EMD-1281.